Gait & Posture 70 (2019) 71–78

Contents lists available at ScienceDirect

Gait & Posture

journal homepage: www.elsevier.com/locate/gaitpost

EEG time-frequency analysis provides arguments for arm swing support in human gait control

Joyce B. Weersink, Natasha M. Maurits, Bauke M. de Jong*

Department of Neurology, University Medical Center Groningen, University of Groningen, Hanzeplein 1, POB 30.001, Groningen, the Netherlands

ARTICLE INFO

Keywords:
Arm swing
Gait cycle
Supplementary motor area (SMA)
Ambulant electroencephalography (EEG)
Event Related Spectral Perturbation (ERSP)

ABSTRACT

Background: Human gait benefits from arm swing, which requires four-limb co-ordination. The Supplementary Motor Area (SMA) is involved in multi-limb coordination. With its location anterior to the leg motor cortex and the pattern of its connections, this suggests a distinct role in gait control.

Research question: Is the SMA functionally implicated in gait-related arm swing?

Methods: Ambulant electroencephalography (EEG) was employed during walking with and without arm swing in twenty healthy subjects (mean age: 64.9yrs, SD 7.2). Power changes across the EEG frequency spectrum were assessed by Event Related Spectral Perturbation (ERSP) analysis over both the putative SMA at electrode position Fz and additional sensorimotor regions.

Results: During walking *with* arm swing, midline electrodes Fz and Cz showed a step-related pattern of Event Related Desynchronization (ERD) followed by Event Related Synchronization (ERS). Walking *without* arm swing was associated with significant ERD-ERS power reduction in the high-beta/low-gamma band over Fz and a power increase over Cz. Electrodes C3 and C4 revealed a pattern of ERD during contralateral- and ERS during ipsilateral leg swing. This ERD power decreased in gait without arm swing (low-frequency band). The ERSP pattern during walking with arm swing was similar at CP1 and CP2: ERD was seen during double support and the initial swing phase of the right leg, while a strong ERS emerged during the second half of the left leg's swing. Walking without arm swing showed a significant power reduction of this ERD-ERS pattern over CP2, while over CP1, ERS during left leg's swing turned into ERD.

Conclusion: The relation between arm swing in walking and a step-related ERD-ERS pattern in the high-beta/low-gamma band over the putative SMA, points at an SMA contribution to integrated cyclic anti-phase movements of upper- and lower limbs. This supports a cortical underpinning of arm swing support in gait control.

1. Introduction

Locomotion of quadrupeds obviously requires coordination between four limbs. Human bipedal gait similarly exhibits a characteristic four-limb pattern, with anti-phase arm swing in the same frequency as the lower limb oscillations. Such arm swing has been suggested to contribute to stabilization [1,2], energetic efficiency [1,3,4], and recruiting neuronal support for maintaining the cyclic motor pattern [5–8].

Gait movements are strongly driven by rhythm generating networks in the spinal cord and brainstem that are, however, crucially embedded in more widely distributed networks also comprising cortical regions [9–13]. The latter enable dynamic involvement of multiple sensory domains in gait control, underscoring the flexibility of underlying motor programs [14]. At the cortical level, the primary motor cortex (M1) and Supplementary Motor Area (SMA) play distinct roles in gait. M1 has been argued to directly drive muscles for steady-state walking [15–21], although the SMA has direct output to the spinal cord too [22–25]. Selective SMA and no M1 activation during imaginary locomotion suggests higher-order involvement of the SMA [26,27]. A characteristic difference between the SMA and M1 that may point at region-specific motor contributions concerns their transcallosal connectivity. The SMA has stronger and more widespread connections with the motor field of the contralateral cortex, compared to M1, supporting the idea that the SMA participates in a more bilateral motor system, indeed serving opposite limb coordination [28,29]. The SMA contribution to walking may also be inferred from lesions resulting in disequilibrium and gait abnormalities [30–33]. In Parkinson's Disease (PD), decreased SMA activation has been associated with gait deficits that become manifest in reduced step length and lost arm swing [34–36]. Notwithstanding the evident role of the SMA in opposite limb

* Corresponding author at: Department of Neurology, University Medical Center Groningen, Hanzeplein 1, P. O. Box 30.001, 9700 RB Groningen, the Netherlands.
E-mail address: b.m.de.jong@umcg.nl (B.M. de Jong).

https://doi.org/10.1016/j.gaitpost.2019.02.017
Received 2 March 2018; Received in revised form 31 January 2019; Accepted 22 February 2019

coordination, this involvement is organized within wider distributed cortical circuitry [37,38]. Aside from its role in upper-limb co-ordination, the SMA plays a pivotal role in voluntary movement initiation [39–43]. This SMA involvement in both bilateral movement coordination and movement initiation thus appears consistent with a central role in circuitry repeatedly pacing the cyclic pattern of four limbs during gait, in which arm swing might serve as a driving force in walking. As the SMA has direct connections to both the spinal cord [22–25] and M1 [44], its proposed role in gait control may be effectuated by either direct input to lower motor centers, input mediated by M1, or both.

Brain activity during overground walking can be studied by ambulant electroencephalography (EEG). With data collected in this manner, functional cortical circuitry underlying stereotypical movement patterns can be identified by calculating Event Related Spectral Perturbations (ERSP), providing an assessment of average dynamic changes in power across the broad band EEG frequency spectrum as a function of time relative to experimental events. Alpha (7–12 Hz), beta (12–30 Hz) and gamma (30+ Hz) oscillations have shown strong movement-related modulations within the motor system [45–49]. Decreases of M1 oscillations in alpha and beta bands prior to and during movement (i.e. ERD) are followed by a post-movement rebound (Event Related Synchronization (ERS)) [50–52], while an intra-stride pattern of activation and deactivation has been demonstrated over the sensorimotor cortex [19]. Particularly the cyclic pattern of hemispheric midline modulations within the low-gamma band has been related to the organization of active walking [53,54].

In the present study, we explored cortical mechanisms involved in the apparent supporting role of arm swing in human gait. We hypothesized that, at the cortical level, particularly activity of the SMA reflects the neuronal organization of such gait supporting arm swing. We therefore employed ERSP to examine, both during overground walking with and without arm swing, involvement of particularly the SMA and M1 leg area, as well as surrounding motor-related cortical regions. With EEG, brain activity during successive stages of the gait cycle was recorded from 32 scalp electrodes. The locations over the SMA (Fz) and M1 leg area (Cz) were the primary focus of this study. In this respect, the occurrence of high-frequency ERD over the SMA preceding ERD over the leg M1, might provide an argument favoring a premotor effect on M1 [55,56]. In addition, recordings at C3, C4, CP1 and CP2 were analyzed. Accelerometry recordings enabled identification of gait phases.

2. Methods

2.1. Participants

Twenty healthy participants (7 males and 13 females, mean age 64.95 years, SD 7.2 years) were included in the study. Their advanced age enabled future reference with patients suffering from neurodegenerative diseases such as PD. None of them suffered from neurological disorders or used medication that influences movement. All participants were able to walk independently and had no cognitive problems (mean mini-mental state exam score 29.15, SD 0.99). They were right handed according to the Annett Handedness scale [57] and gave their written informed consent. The study was executed according to the Declaration of Helsinki (2013) and was approved by the ethical committee of the University Medical Center Groningen.

2.2. Task and experimental set-up

The experiment consisted of two sessions conducted on the same day with approximately 10 min in between. Participants were instructed to walk at their own comfortable speed through a hallway of 150 m in a straight line from start to finish and back. Turning was not included in the analysis. The first sessions was always walking with arm swing, i.e. participants were asked to walk as they would do when taking a walk in the park. This instruction aimed to avoid that participants would become highly aware of their arm swing with the risk of blocking gait with natural (anti-phase) arm swing. The second session was without arm swing, which implied that participants were instructed to keep their arms aligned with their body. Afterwards, video recordings were used to check whether participants did not accidentally swing their arms. During the two sessions, monopolar EEG was recorded using a cap with 32 active Ag-AgCl electrodes (EasyCap GmbH, Herrsching, Germany) located according to the international 10–20 system. With these electrodes, amplification first takes place at the electrode, thereby considerably suppressing potential artifacts in the EEG recordings due to cable movements. The ground and reference electrodes were located between Fz and FCz and between Cz and Fz, respectively. To further limit artifacts in the EEG, participants were asked to relax face and jaw muscles and to minimize eye blinks and swallowing during data recording, as much as possible. To mark the times of 'Heel Strike' and lifting the toe from the floor (Toe-Off) during walking, a tri-axial accelerometer (Compumedics Neuroscan, Singen, Germany) was placed over the L3 segment of the lumbar spine over the clothes, using Velcro straps. For this trunk accelerometer, the orientation of the three accelerometer axes, X, Y, and Z, when standing in the anatomical position, was medial/lateral, superior/inferior, and anterior/posterior, respectively. Positive X-values thus corresponded to acceleration to the left, positive Y-values to upward acceleration and positive Z-values to forward acceleration. The EEG and accelerometer signals were recorded and synchronized at a sampling rate of 1024 Hz using a portable amplifier (Siesta, Compumedics Neuroscan, Singen, Germany) and sent via WIFI to Profusion EEG software (v. 5.0, Compumedics Neuroscan, Singen, Germany) on a laptop and stored for later analysis.

2.3. Gait analysis

The exact time-points of Heel Strike and Toe-Off were determined by an approach introduced by Sejdic et al. (2016) [58]. The algorithm based on their work has three stages. In the first stage, the Y direction signal is used to identify potential gait events. Here, the time-points of maximum positive accelerometer amplitude in the Y direction were selected. These points were used in the second stage to identify Toe-Off. Based on the average value of the first 10 ms following the point selected in stage 1 of a leg accelerating in the X direction, the algorithm determined whether a step was made with the left or right leg. In the second stage, potential events from the first stage were processed to identify true Toe-Off for the left and right foot. These true events are characterized by the first negative peak after the largest positive peak in the Y direction, which was selected in the first stage. In the final (third) stage, the first negative peak before the largest positive peak in the Z direction of the accelerometer data was selected, which determines the Heel-Strike events. These three stages enable establishing the exact time-points of left and right Heel-Strike as well as left and right Toe-Off. These time-points were used to calculate swing time and stride time (of the full motion cycle) and served as markers for EEG analysis. The final stage of standing on a leg preceding the swing phase is the phase of double support, demarcated by opposite Heel Strike and Toe-Off. To determine gait variability, we calculated the stride time coefficient of variation by dividing the stride time standard deviation by the mean stride time across both walking sessions for each participant [59,60]. Moreover, as an index of gait symmetry, swing time symmetry ratio was calculated by dividing the mean left swing time by the mean right swing time [61].

2.4. Data pre-processing and analysis

Pre-processing and analyses were performed in MATLAB2014a (The MathWorks) using EEGLAB 13_1_1b (sccn.ucsd.edu/eeglab), an open source environment for processing electrophysiological data. EEG

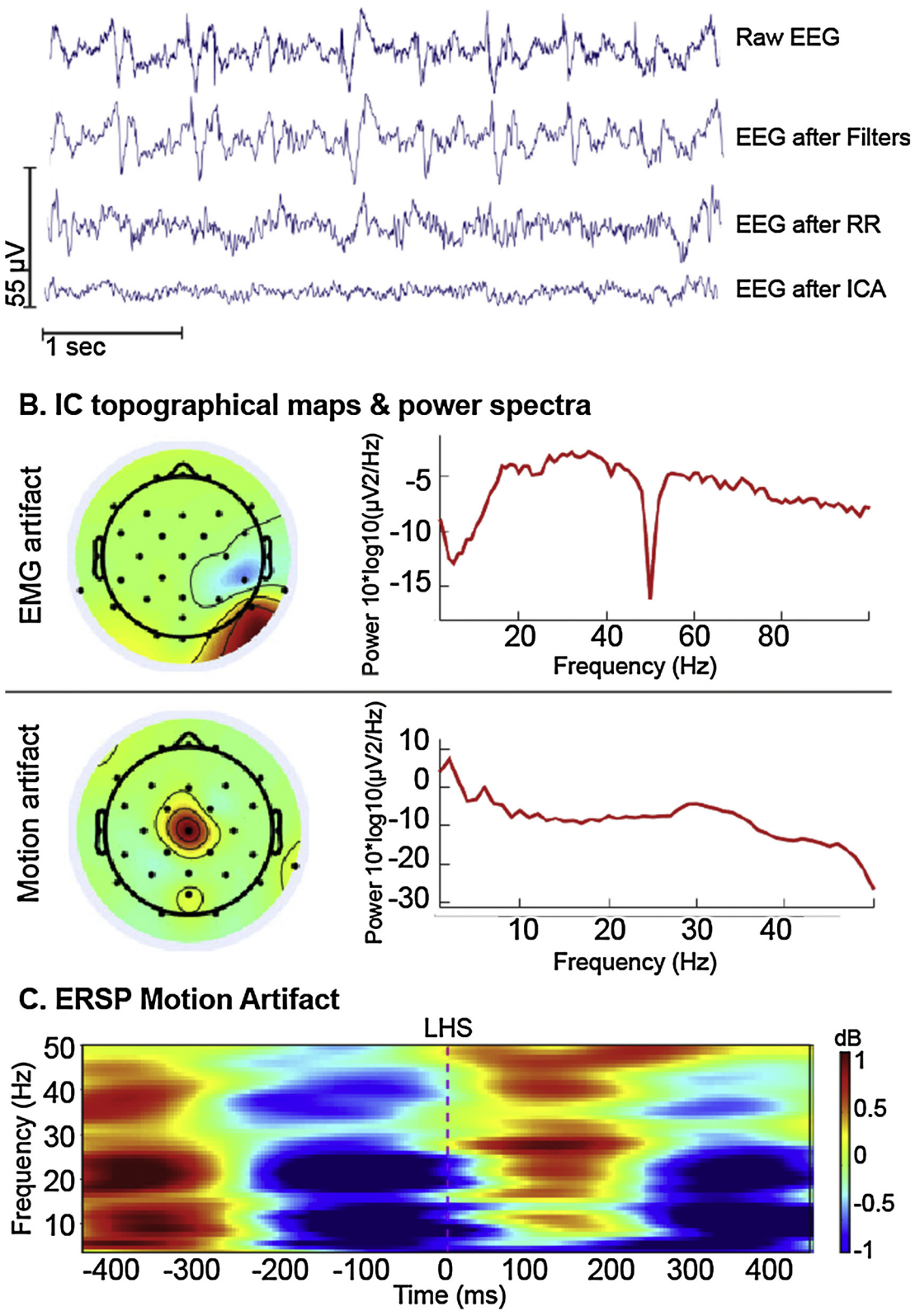

(caption on next page)

Fig. 1. Preprocessing of EEG data.
(A) EEG data at Cz for a single subject before and after successive preprocessing steps, illustrated from top to bottom: Raw data, EEG after filtering (finite impulse response high pass filter with a cut-off at 1 Hz and Notch filter at 50 and 100 Hz), EEG after rereferencing to average and EEG after subsequent independent component analysis (ICA).
(B) Topographical maps and power spectra of typical excluded independent components representing EMG and motion artifacts.
(C) Event related spectral perturbation (ERSP) plot of an excluded independent component representing gait related motion artifacts. Event related desynchronization (ERD) is illustrated in blue, event related synchronization (ERS) in red.
Abbreviations; EEG = Electroencephalography; RR = Re-referencing; ICA = Independent Component Analysis; EMG = Electromyography; IC = Independent Components; ERSP = Event Related Spectral Perturbation; LHS = Left Heel Strike; dB = decibel.

recordings during overground walking were truncated to the straight-line walking segments (starting, stopping and turning segments were removed). To speed up computations the data were down sampled offline to a sampling rate of 256 Hz. Data were high pass filtered at 1 Hz using a finite impulse response (FIR) filter (Fig. 1A) with zero phase shift and also filtered for removing line noise at 50 and 100 Hz using the Cleanline technique (nitrc.org/projects/cleanline/). The next step concerned removing channels exhibiting substantial artifacts using the following criteria: (1) channels with magnitude < 30 or > 10.000 μV; (2) channels with kurtosis > 5 standard deviations from the mean; (3) channels uncorrelated with the neighbouring channels ($r < 0.4$) for more than 1% of the total time; (4) channels with standard deviation qualitatively higher than the other channels. These cutoffs were based on the work of Gwin and colleagues [62]. Data were subsequently re-referenced to the average of the remaining channels, which has been shown to minimize motion artefacts in EEG signals when performed as a post-processing step [63]. EEG data were epoched from 1000 ms before until 1000 ms after time of LHS. Infomax ICA was applied on the cleaned data sets to transform the EEG channel data into temporally independent component signals. DIPFIT functions within EEGLAB [64] computed an equivalent current dipole model that best explained the scalp topography of each IC using a boundary element head model based on the Montreal Neurological Institute (MNI) template (the average of 152 MRI scans from healthy subjects, available at http://www.mni.mcgill.ca). ICs were excluded from the data for further analysis if the projection of the equivalent current dipole model to the scalp accounted for less than 80% of the scalp map variance [65], or if the topography and time-course of the IC was reflective of eye movement artifact [66,67]. Remaining ICs were classified as electrocortical sources or muscle sources based on inspection of their power spectra, ERSP and locations of their equivalent current dipoles. Spectral power peaks at stride frequency and broadband synchronization and desynchronization assisted in identifying ICs that were primarily related to movement artifacts rather than electrocortical activity (as illustrated in Fig. 1B–C). One last visual inspection was performed to check the quality of the cleaned data.

Afterwards, the complete dataset was split into segments of interest from the moment of Heel Strike until 1000 ms after. Between 120 and 150 epochs were used for the ERSP analysis for each participant. For each participant, the initial and final five gait cycles were removed to eliminate irregularity due to acceleration and delay at the onset and end of walking in the hallway. Single trial spectrograms were computed for each subject and channel and subsequently time-warped (to mean step latencies) using a linear interpolation function, to align the time-points for the right and left heel strikes over epochs following the methods by Gwin and colleagues [62].

To calculate gait cycle ERSPs the gain model was used [68], which is the default mode in EEGLAB. In this model, event-related spectral power changes were analyzed by the ERSP index:

$$ERSP(f, t) = \frac{1}{n}\sum_{k=1}^{n} (F_k(f, t))^2$$

where for n trials, $F_k(f,t)$ is the spectral estimate of trial k at frequency f and time t. ERSP shows mean time-frequency points across the input epochs, where higher or lower spectral power differs from mean power during the 1000 ms pre-stimulus baseline period of the same epochs, i.e. the mean of an entire gait cycle. The grand average mean ERSP plots for C3, C4, CP1, CP2, Cz and Fz for both walking with and without arm swing were generated. The color at each image pixel then indicates power (in dB) at a given frequency and latency relative to the time locking event.

To provide additional insight in the results from the elaborate analysis performed on selectively the recording sites Fz, Cz, C3, C4, CP1 and CP2, 32-channel ERSP scalp distribution maps of both low and high frequency ranges were made for the two walking conditions.

2.5. Statistical analysis

Pooled ERSP and significant ERSP differences between walking with and without arm swing were identified using a nonparametric bootstrapping method corrected for multiple comparisons using the False Discovery Rate (FDR) method available within EEGLAB 13_1_1b. SPSS version 23 for Windows (IBM Japan Ltd., Tokyo, Japan) was used for statistical analysis of gait characteristics. For normally distributed data, i.e. swing time symmetry ratio and stride time coefficient of variation, a paired *t*-test was used and for non-normally distributed data, i.e. stride time, a Wilcoxon signed rank test was used to compare walking with and without arm swing. An alpha level of 0.05 was assumed.

3. Results

3.1. Gait characteristics

Compared to walking with arm swing, walking without resulted in an 8.8% larger stride time coefficient of variation which was, however, not a statistically significant difference (Table 1). Neither did the small differences (1–2%) in the stride time and swing time symmetry ratio reach statistical significance.

3.2. Event related spectral perturbations

3.2.1. Recordings at Fz (putative supplementary motor area) and Cz (putative motor cortex – legs)

For both walking conditions, the recordings at the midline sites Fz and Cz showed a well-demarcated pattern of an ERD-ERS alternation within each step, most pronounced in the 5–12 Hz range, which thus corresponded with the periodicity of the gait cycle (mean cadence of 55

Table 1
Gait characteristics for both walking with and without arm swing, obtained by accelerometer recording. The normally distributed and non-normally distributed characteristics are reported as mean ± standard deviation and median ± interquartile range, respectively. Statistical analysis was performed using paired *T*-test for normally and Wilcoxon signed rank test for non-normally distributed characteristics. STCV = Stride time coefficient of variation, STSR = swing time symmetry ratio, l = left, r = right. IQR = interquartile range, SD = standard deviation.

	Walking with arm swing	Walking without arm swing	P-value
Stride time (s)	1,095 (IQR 0,090)	1,075 (IQR 0,080)	0.145
STCV (%)	3,043 (SD 0,986)	3,313 (SD 1,538)	0.461
STSR (l/r)	0,998 (SD 0,050)	0,987 (SD 0,051)	0.483

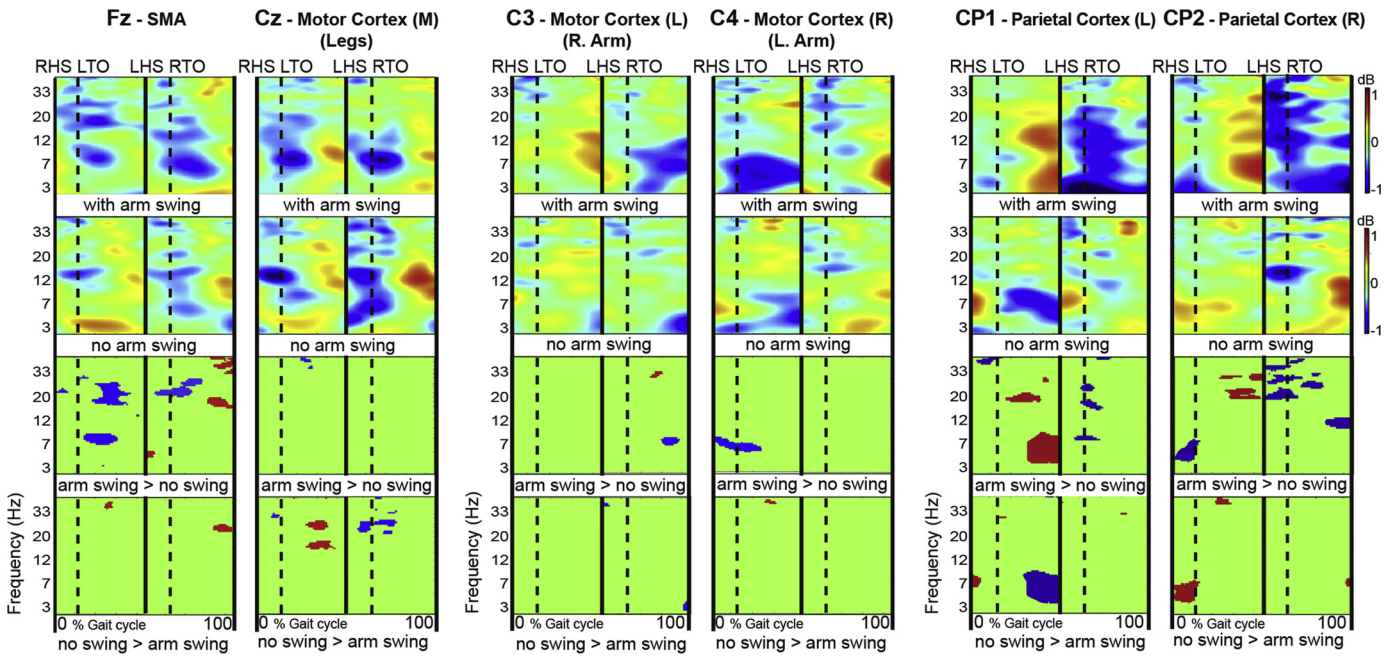

Fig. 2. Group averaged gait related ERSP plots.

Dynamic changes across the EEG frequency spectrum from electrodes over the putative Supplementary motor Area (SMA), motor cortex representing both legs and left and right arm and the left and right parietal cortex during the successive stages of the gait cycle while walking with armswing and without armswing. The stage between heel strike and lifting the toe of the opposite leg from the floor, demarcates the phase of double support in which the swing phase is prepared. In the upper two images blue illustrates Event related desynchronization (ERD) and red represents event related synchronization (ERS). Significant differences ($p < 0.05$) per electrode between the two walking modes are shown in the bottom two images. Red represents a significant power increase in ERS, blue a significant power increase in ERD.

Abbreviations: ERSP = Event Related Spectral Perturbations; dB = decibel; RHS = Right Heel Strike; LTO = Left Toe Off; LHS = Left Heel Strike; RTO = Right Toe Off.

strides/minute). In the swing phase of each leg, a strong ERD emerged around Toe-Off until the mid-swing phase, followed by a transition to ERS that lasted in the final part of the swing phase (Fig. 2). The ERS was stronger at Cz than at Fz. Although this alternating ERD-ERS pattern in the low (5–12) Hz range was seen in both gait conditions, it was more pronounced in walking with, compared to walking without swing. Particularly at Fz, ERD power in this low frequency range decreased during walking without arm swing.

In the 15–30 Hz frequency range at Fz, an alternating ERD-ERS pattern that resembled the pattern in the lower frequency range was only seen for walking with arm swing. Walking without arm swing revealed a significant power reduction in particularly the initial ERD for these higher frequencies, compared to walking with arm swing ($p = 0.012$) (Fig. 2). For the 15–30 Hz frequency range at Cz (the estimated location over the M1 leg area) this alternating ERD-ERS pattern was only slightly recognized when walking with arm swing. At Cz, however, walking without arm swing revealed an opposite effect, i.e. a significant increase of power occurred in this high-frequency range in both ERD and ERS ($p = 0.031$). This enhanced ERD and ERS was present around the (right) Toe-Off and during the left mid-swing phase, respectively (Fig. 2).

3.2.2. *Recordings at C3 and C4 (putative left and right motor cortex - arms)*

While at Cz, a consistent ERD-ERS succession was observed *within* the swing phase of each leg (5–12 Hz range), recordings at C3 and C4 showed that walking with arm swing was related with a pattern of alternating ERD and ERS, each related to the swing phase of opposite legs (Fig. 2). At C3 (putative left motor cortex representation of the right arm), the entire swing phase of the right leg showed a strong ERD (in the 5–12 Hz range), thus corresponding with the back swing of the right arm, while ERS was seen during the second half of the swing phase of the left leg, corresponding with the final stage of the right arm's forward swing. In the 5–12 frequency range at C4 (putative right motor cortex representation of the left arm), the entire swing phase of the left leg showed a strong ERD, thus corresponding with the back swing of the left arm, while ERS during the second half of the right leg's swing phase corresponded with the final stage of the left arm's forward swing. During walking without arm swing, power of the strong ERD that corresponded with the back swing of the contralateral arm was significantly reduced in the 5–12 frequency range, both at C3 and C4 ($p = 0.022$ and $p = 0.024$, respectively) (Fig. 2).

In the high-frequency range (15–50 Hz), walking with arm swing showed a less pronounced pattern characterized by ERD around Toe-Off for each leg at C3 as well as C4, followed by ERS towards the end of the leg's swing phase. This pattern in the 15–50 frequency range did not significantly change during walking without arm swing (Fig. 2).

3.2.3. *Recordings at CP1 and CP2 (putative left and right parietal cortex)*

Walking with arm swing showed broadband ERSP dynamics of which the temporal pattern was largely similar at CP1 and CP2: strong ERD occurred around right Toe-off and a strong ERS was seen in the second half of the swing phase of the left leg (Fig. 2). Leg movements in these phases of the gait cycle generally correspond with upper limb movements in the transition to right-arm back swing and the final part of the left-arm back swing. This pattern virtually comprised the entire frequency range, with the exception that it was less pronounced in the 30–50 Hz frequency range at CP1. Moreover, in the very low frequency range (< 5 Hz), the ERD extended in both the double support and entire right-leg swing phase of the gait cycle.

During walking without arm swing, the clear demarcation between ERD and ERS that was seen over a wide frequency range during walking with arm swing disappeared. In the 15–50 Hz frequency range at particularly CP2, without arm swing, ERD power significantly decreased at the transition from double support to the right-leg swing phase

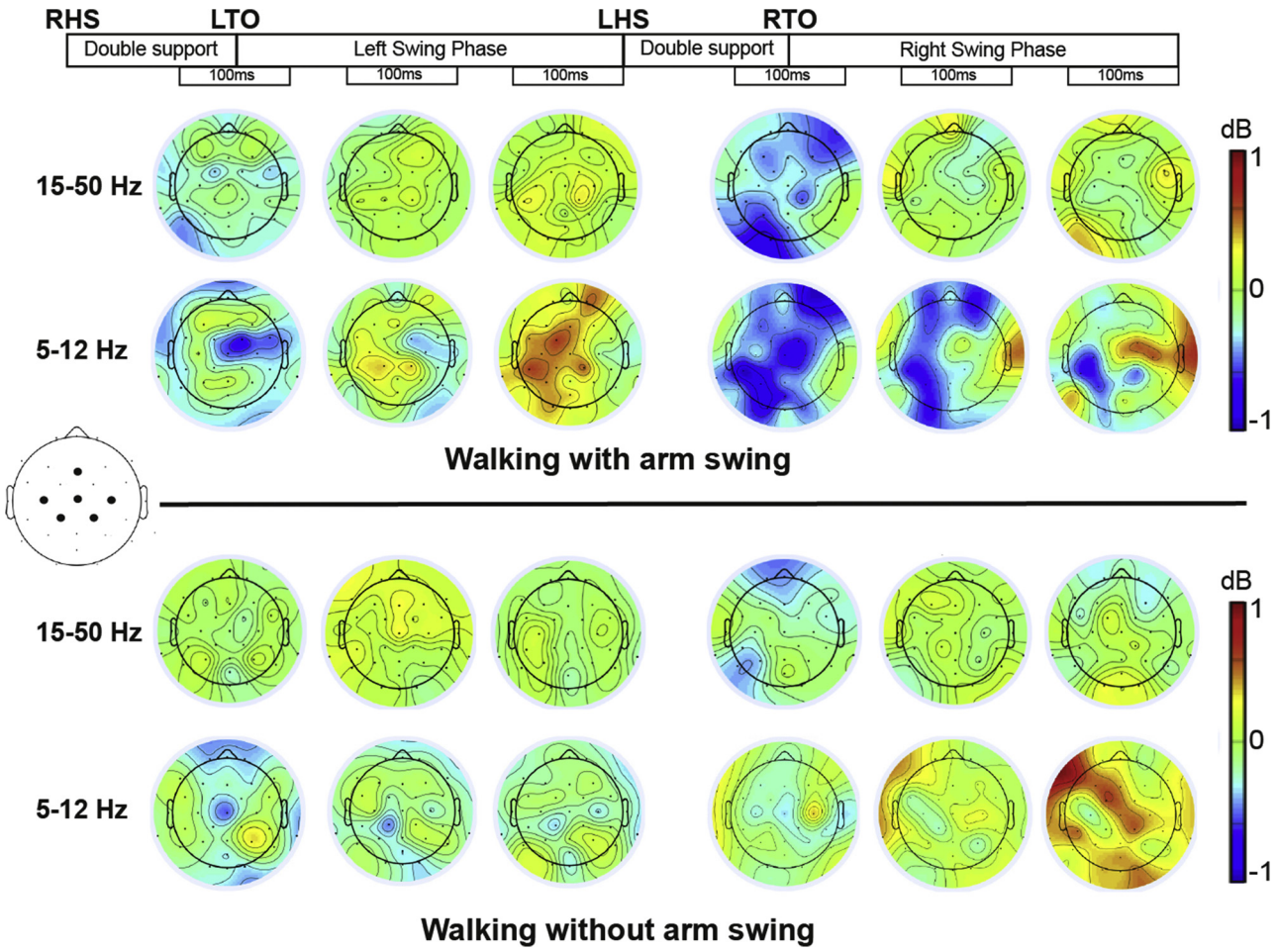

Fig. 3. ERSP scalp distribution maps.
Topographic distribution of the ERSP over the entire scalp (32 channels) for walking with and without arm swing, in high frequency (15–50 Hz) and low frequency (5–12 Hz) ranges. Within the gait cycle, 100 ms epochs were selected from the Toe-Off, mid swing and end swing phases. Event related desynchronization (ERD) is illustrated in blue, event related synchronization (ERS) in red.
Abbreviations: see legends of Fig. 2.

($p = 0.013$), while ERS power decreased in the second half of the left-leg swing phase ($p = 0.048$) (Fig. 2). At CP1, such decreases were more subtle. In other words, parietal ERSP in the high frequency range related to (bilateral) arm swing in gait appeared to be predominantly right-lateralized.

In the 5–10 Hz frequency range at CP2, during walking without arm swing, ERD turned into ERS in the double support phase preceding left Toe-off, compared to walking with arm swing ($p = 0.001$) (Fig. 2). The opposite was seen in the second half of the left leg's swing phase at CP1: ERS turned into ERD during walking without arm swing, compared to gait with arm swing ($p = 0.007$).

3.3. ERSP scalp maps

The spatial distribution of ERSP over the entire scalp during walking with and without arm swing provided additional information to complement optimal assessment of the ERSP plots presented for Cz, Fz, C3, C4, CP1 and CP2 (Fig. 3).

4. Discussion

In the present study we found characteristic differences between walking with and without arm swing regarding the electrocortical activity recorded at Fz and Cz, putatively representing (and further referred to as) the SMA and the leg area of M1, respectively. These differences provide support for a specific contribution of the SMA in overground walking with natural arm swing. The regular within-step ERD-ERS succession that was identified over both midline areas during walking with arm swing is generally consistent with the literature [11,19,69,70]. While in the lower (5–12 Hz) frequency range, the within-step ERD-ERS succession remained essentially unaffected over the leg M1 during walking without arm swing, this condition without arm swing showed a less sharply demarcated ERD-ERS pattern (with significantly reduced ERD) over the more anteriorly located SMA. Moreover, in the higher frequency range (15–50 Hz), this regular ERD-ERS pattern related to walking with arm swing was clearly identified over the SMA and not over the leg M1, while particularly the ERD power of this pattern over the SMA was significantly stronger in walking with arm swing compared to walking without. At the contrary, in this higher frequency range, ERSP power over the leg M1 became stronger during walking without, compared to walking with arm swing.

This arm swing-related ERSP power may thus represent the contribution of the SMA to efficient four-limb movement, while in the absence of arm swing, stronger high-frequency power over the leg M1 might point at enhanced effort to organize the legs cyclic movement pattern [53]. In walking with arm swing the observed ERD over the SMA did not precede the leg M1 ERD, which implies that our measurements did not provide arguments for a crucial influence of the SMA on M1 [55,56]. Further support for the involvement of the SMA in four-limb co-ordination can be inferred from the observation that at the C3

and C4 recordings, representing the more lateral left and right motor cortex, respectively, no characteristic step-related ERD-ERS pattern was observed. Instead, we found a strong low-frequency ERD that lasted during the entire swing phase of the contralateral leg. This contralateral forward leg swing corresponds in time with a back swing of the arm on the same side. Decrease of the ERD at these recording sites during walking without arm swing could thus be related to reduced back swing of the contralateral arm [71]. In contrast to the ERD changes over the SMA, however, the profile of strictly contralateral ERD over the motor cortex is an argument against a specific contribution to bilateral motor control. We acknowledge that, although the lateral position of C3 and C4 supports a stronger relation with arm than leg movement, an absolute dissociation cannot be proven from our data. Indeed, enhanced ERD has been previously observed over the more lateral motor cortex during active walking compared to passive walking, both without arm swing [53].

A third characteristic ERSP pattern was observed at the two parietal recording sites CP1 (left) and CP2 (right). Here, during walking with arm swing, ERSP analyses suggests a lateralized movement phenomenon: around the onset of the swing phase of the right leg, a strong ERD emerged over both parietal regions, following the abrupt ending of a strong ERS at left heel strike. A weak ERD around the onset of left leg swing was only found over the right and not the left parietal cortex. An unequivocal explanation is hard to give. The parietal ERD onset precedes the ERD recorded over the above described regions, which might suggest a higher-order motor component providing information for the SMA and motor cortex [56,72]. As this bilateral parietal ERD occurs around the onset of particularly right leg movement, one might infer that such information is specifically channeled to the (dominant) left motor cortex. Given the sharp transition from ERS to ERD at left heel strike, which is most striking over the right parietal cortex, such parietal information might include a sensory trigger for the preparation of (dominant) right leg movement [73–75]. The involvement of coinciding arm and leg movements, in anti-phase, associated with both motor and sensory neuronal activations illustrates the complexity of possible parietal mechanisms. Nevertheless, it is intriguing to see that the ERS–ERD power in the high frequency range around left heel strike is significantly reduced over the right parietal cortex when walking without arm swing. In this respect one might speculate that arm swing also provides a sensory contribution gait control.

In PD, a typical characteristic of affected gait is the absence of arm swing [34–36], a symptom that emerges together with problems in gait initiation. These features are both seen as a consequence of impaired SMA function due to reduced input from affected cortico-basal ganglia loops [34,76]. Gait disturbances in a disease characterized by SMA dysfunction are thus consistent with our results from healthy subject that point at a contribution of arm swing to efficient walking, mediated by the SMA. This cortical role in walking is complementary to, and not at odds with integration between cyclic movement patterns of upper and lower limbs embedded in e.g. spinal cord circuitry [7,8]. Although the stride time coefficient of variation was larger in walking without arm swing, we did not find significant differences between the behavioral characteristics of walking with and without arm swing. In this respect, a reduced contribution of the SMA to efficient four-limb coordination may be compensated by the enhanced impact of M1 activity of the legs, as proposed above.

With regard to the experimental design of the present study, one might question whether the instruction of walking without arm swing may inflict an unnatural, more conscious and variable gait which introduces an additional component in the EEG power modulations [11]. Given the easy task, we do not consider this to be a confounding effect. Another methodological issue is that ambulatory 32-channel EEG remains susceptible to and is limited in extracting specifically movement artefacts, which requires cautious data preprocessing and critical evaluation of EEG phasic changes [19,77–79].

5. Conclusion

EEG and accelerometer data recorded during walking demonstrated coherent cyclic changes of power in distinct EEG frequency bands over the SMA and M1 leg area. These patterns support the conclusion that, during overground walking, arm swing-associated activity over the SMA represents a neuronal organization that contributes to integrated cyclic anti-phase movements of the upper- and lower limbs. As we did not find arguments from the temporal succession of ERSP patterns that the SMA facilitates M1 to generate motor commands for locomotion, a plausible mechanism includes a direct SMA effect on the spinal cord. The ERSP analysis thus provides a neuronal underpinning of arm swing support in walking and highlights a cortical contribution. Better understanding of both bottom-up and top-down pathways coordinating movements of the four limbs during gait may serve rehabilitation concepts concerning impaired walking in neurological conditions such as PD, spinal cord injury and stroke.

Declaration of interest

None.

References

[1] J. Ortega, L. Fehlman, C. Farley, Effects of aging and arm swing on the metabolic cost of stability in human walking, J. Biomech. 41 (2008) 3303–3308.
[2] A. Hof, The equations of motion for a standing human reveal three mechanisms for balance, J. Biomech. 40 (2007) 451–457.
[3] B. Umberger, Effects of suppressing arm swing on kinematics, kinetics, and energetics of human walking, J. Biomech. 41 (2008) 2575–2580.
[4] Z. Yizhar, S. Boulos, O. Inbar, E. Carmeli, The effect of restricted arm swing on energy expenditure in healthy men, Int. J. Rehabil. Res. 32 (2009) 115–123.
[5] D.P. Ferris, H.J. Huang, P. Kao, Moving the arms to activate the legs, Exerc. Sport Sci. Rev. 34 (2006) 113–120.
[6] H.J. Huang, D.P. Ferris, Neural coupling between upper and lower limbs during recumbent stepping, J. Appl. Physiol. 97 (2004) 1299–1308.
[7] F. Massaad, O. Levin, P. Meyns, D. Drijkoningen, S.P. Swinnen, J. Duysens, Arm sway holds sway: locomotor like modulation of leg reflexes when arms swing in alternation, Neuroscience 258 (2014) 34–46.
[8] N. Kawashima, D. Nozaki, M.O. Abe, K. Nakazawa, Shaping appropriate locomotive motor output through interlimb neural pathway within spinal cord in humans, J. Neurophysiol. 99 (2008) 2946–2955.
[9] S. Rossignol, J. Dubuc, J. Gossard, Dynamic sensorimotor interactions in locomotion, Physiol. Rev. 86 (2006) 89–154.
[10] K. Takakusaki, Neurophysiology of gait: from the spinal cord to the frontal lobe basic framework of locomotor control spinal locomotor network generates basic locomotor pattern, Mov. Disord. 28 (2013) 1483–1491.
[11] J. Wagner, T. Solis-Escalante, R. Scherer, C. Neuper, G. Müller-Putz, It's how you get there: walking down a virtual alley activates premotor and parietal areas, Front. Hum. Neurosci. 8 (2014) 1–11.
[12] B. Lau, M. Welter, H. Belaid, S.F. Vidal, E. Bardinet, D. Grabli, C. Karachi, The integrative role of the pedunculopontine nucleus in human gait, Brain 138 (2015) 1284–1296.
[13] F. Mori, K. Okada, T. Nomura, Y. Kobayashi, The pedunculopontine tegmental nucleus as a motor and cognitive interface between the cerebellum and basal ganglia, Front. Neuroanat. 10 (2016) 1–8.
[14] F. Lacquaniti, Y.P. Ivanenko, M. Zago, Patterned control of human locomotion, J Physiol 10 (2012) 2189–2199.
[15] F. Artoni, C. Fanciullacci, F. Bertolucci, A. Panarese, S. Makeig, S. Micera, C. Chisari, Unidirectional brain to muscle connectivity reveals motor cortex control of leg muscles during stereotyped walking, Neuroimage 159 (2017) 403–416.
[16] B.J. Farrell, M.A. Bulgakova, I.N. Beloozerova, M.G. Sirota, B.I. Prilutsky, Body stability and muscle and motor cortex activity during walking with wide stance, J. Neurophysiol. 112 (2014) 504–524.
[17] T.H. Petersen, M. Willerslev-Olsen, B.A. Conway, J.B. Nielsen, Motor cortex drives the muscles during walking in human subjects, J. Physiol. 10 (2012) 2443–2452.
[18] C. Iglesias, G. Lourenco, V. Marchand-pauvert, Weak motor cortex contribution to the quadriceps activity during human walking, Gait Posture 35 (2012) 360–366.
[19] J.T. Gwin, K. Gramann, S. Makeig, D.P. Ferris, Electrocortical activity is coupled to gait cycle phase during treadmill walking, Neuroimage 54 (2011) 1289–1296.
[20] N.L. Hansen, S. Hansen, L.O. Christensen, N.T. Petersen, J.B. Nielsen, Synchronization of lower limb motor unit activity during walking in human subjects, J. Neurophysiol. 86 (2001) 1266–1276.
[21] C. Capaday, B.A. Lavoie, H. Barbeau, C. Schneider, B.A. Lavoie, H. Barbeau, Studies on the corticospinal control of human walking. I. Responses to focal transcranial magnetic stimulation of the motor cortex, Am. Physiol. Soc. 99 (1999) 129–139.
[22] S. He, R. Dum, P. Strick, Topographic organization of corticospinal projections from the frontal lobe: motor areas on the medial surface of the hemisphere, J. Neurosci.

15 (1995) 3284–3306.
[23] M.A. Maier, J. Armand, P.A. Kirkwood, H.W. Yang, J.N. Davis, R.N. Lemon, Differences in corticospinal projection from primary motor cortex and supplementary motor area to macaque upper limb motoneurons: an anatomical and electrophysiological study, Cereb. Cortex 12 (2002) 281–296.
[24] S. Vaalto, L. Säisänen, M. Könönen, P. Julkunen, T. Hukkanen, S. Määttä, J. Karhu, Corticospinal output and cortical excitation inhibition balance in distal hand muscle representations in nonprimary motor area, Hum. Brain Mapp. 32 (2011) 1692–1703.
[25] S. Teitti, S. Määttä, L. Säisänen, M. Könönen, R. Vanninen, H. Hannula, E. Mervaala, J. Karhu, Non primary motor areas in the human frontal lobe are connected directly to hand muscles, Neuroimage 40 (2008) 1243–1250.
[26] I. Miyai, H.C. Tanabe, I. Sase, H. Eda, I. Oda, I. Konishi, Y. Tsunazawa, Cortical mapping of gait in humans: a near-infrared spectroscopic topography study, Neuroimage 1192 (2001) 1186–1192.
[27] C. La Fougere, A. Zwergal, A. Rominger, S. Förster, G. Fesl, M. Dieterich, T. Brandt, M. Strupp, P. Bartenstein, K. Jahn, Real versus imagined locomotion: a [18 F] -FDG PET-fMRI comparison, Neuroimage 50 (2010) 1589–1598.
[28] E.M. Rouiller, A. Babalian, O. Kazennikov, V. Moret, X.H. Yu, M. Wiesndanger, Transcallosal connections of the distal forelimb representations of the primary and supplementary motor cortical areas in macaque monkeys, Exp. Brain Res. 102 (1994) 227–243.
[29] K.L. Ruddy, A. Leemans, R.G. Carson, Transcallosal connectivity of the human cortical motor network, Brain Struct. Funct. 222 (2017) 1243–1252.
[30] Sala S. Della, A. Francescani, H. Spinnler, Gait apraxia after bilateral supplementary motor area lesion, J Neurol Neurosurg Psychiatry 41 (2002) 77–85.
[31] S.E. Nadeau, Gait apraxia: further clues to localization, Eur. Neurol. 1197 (2007) 142–145.
[32] V.S. Gurfinkel, A.M. El'ner, Contribution of the frontal lobe secondary motor area to organization of postural components in human voluntary movement, Plenum Publ. Corp. 20 (1988) 7–15.
[33] F. Viallet, J. Massion, R. Massarino, R. Khalil, Coordination between posture and movement in a bimanual load lifting task: putative role of medial frontal region including the supplementary motor area, Exp. Brain Res. 88 (1992) 674–684.
[34] I.H. Jenkins, S.W. Fernandez, E.D. Playford, A.J. Lees, Impaired activation of the supplementary motor area in Parkinson's disease is reversed when akinesia is treated with apomorphine, Am. Neurol. Assoc. 32 (1992) 749–757.
[35] M. Jahanshahi, H. Jenkins, R.G. Brown, C.D. Marsden, R.E. Passingham, D.J. Brooks, Self-initiated versus externally triggered movements I. An investigation using measurement of regional cerebral blood flow with PET and movement-related potentials in normal and Parkinson' s disease subjects, Brain (1995) 913–933.
[36] U. Sabatini, K. Boulanouar, N. Fabre, F. Martin, C. Carel, C. Colonnese, L. Bozzao, I. Berry, J.L. Montastruc, F. Chollet, O. Rascol, C.O. Rascol, L. De, Cortical motor reorganization in akinetic patients with Parkinson' s disease A functional MRI study, Brain 123 (2000) 394–403.
[37] F. Debaere, S.P. Swinnen, E. Be, S. Sunaert, P. Van Hecke, J. Duysens, Brain areas involved in interlimb coordination: a distributed network, Neuroimage 958 (2001) 947–958.
[38] D.J. Serrien, The neural dynamics of timed motor tasks: evidence from a synchronization-continuation paradigm, Eur. J. Neurosci. 27 (2008) 1553–1560.
[39] R. Cunnington, C. Windischberger, L. Deecke, E. Moser, The preparation and readiness for voluntary movement: a high-field event-related fMRI study of the Bereitschafts-BOLD response, Neuroimage 20 (2003) 404–412.
[40] L. Deecke, H.H. Kornhuber, An electrical sign of participation of the mesial' supplementary' motor cortex in human voluntary finger movement con prec ips prec con par ips par, Brain Res. 159 (1978) 473–476.
[41] G. Goldberg, Supplementary motor area structure and function: review and hypotheses, Behav. Brain Sci. 8 (1985) 567–616.
[42] C. Sahyoun, A. Floyer-Lea, H. Johansen-Berg, P.M. Matthews, Towards an understanding of gait control : brain activation during the anticipation, preparation and execution of foot movements, Neuroimage 21 (2004) 568–575.
[43] S. Yazawa, H. Shibasaki, A. Ikeda, K. Terada, T. Nagamine, Cortical mechanism underlying externally cued gait initiation studied by contingent negative variation, Electroencephalogr. Clin. Neurophysiol. 105 (1997) 390–399.
[44] G. Luppino, M. Matelli, R. Camarda, G. Rizzolatti, Corticocortical connections of Area F3 (SMA-Proper) and Area F6 (Pre-SMA) in the macaque monkey, J. Comp. Neurol. 338 (1993) 114–140.
[45] S. Ohara, T. Mima, K. Baba, A. Ikeda, T. Kunieda, R. Matsumoto, J. Yamamoto, M. Matsuhashi, T. Nagamine, K. Hirasawa, T. Hori, T. Mihara, N. Hashimoto, S. Salenius, H. Shibasaki, Increased synchronization of cortical oscillatory activities between human supplementary motor and primary sensorimotor areas during voluntary movements, J. Neurosci. 21 (2001) 9377–9386.
[46] B. Pollok, J. Gross, G. Aschersleben, A. Schnitzler, The cerebral oscillatory network associated with auditorily paced finger movements, Neuroimage 24 (2005) 646–655.
[47] J. Gross, B. Pollok, M. Dirks, L. Timmermann, M. Butz, A. Schnitzler, Task-dependent oscillations during unimanual and bimanual movements in the human primary motor cortex and SMA studied with magnetoencephalography, Neuroimage 26 (2005) 91–98.
[48] D. Cheyne, S. Bells, P. Ferrari, W. Gaetz, A.C. Bostan, Self-paced movements induce high-frequency gamma oscillations in primary motor cortex, Neuroimage 42 (2008) 332–342.
[49] S. Houweling, A. Daffertshofer, B.W. Van Dijk, P.J. Beek, Neural changes induced by learning a challenging perceptual-motor task, Neuroimage 41 (2008) 1395–1407.
[50] G. Pfurtscheller, F.H. Lopes, Event-related EEG/ MEG synchronization and desynchronization: basic principles, Clin. Neurophysiol. 110 (1999) 1842–1857.
[51] A.K. Engel, P. Fries, Beta-band oscillations — signalling the status quo? Curr. Opin. Neurobiol. 20 (2010) 156–165.
[52] W. Klimesch, P. Sauseng, S. Hanslmayr, EEG alpha oscillations: the inhibition – timing hypothesis, Brain Res. Rev. 3 (2006) 63–88.
[53] J. Wagner, T. Solis-escalante, P. Grieshofer, C. Neuper, G. Müller-putz, R. Scherer, Level of participation in robotic-assisted treadmill walking modulates midline sensorimotor EEG rhythms in able-bodied subjects, Neuroimage 63 (2012) 1203–1211.
[54] M. Seeber, S. Reinhold, J. Wagner, T. Solis-Escalante, G. Muller-Putz, EEG beta suppression and low gamma modulation are different elements of human upright walking, Front. Hum. Neurosci. 8 (2014) 1–9.
[55] H. Sun, T. Blakely, F. Darvas, J. Wander, L. Johnson, D. Su, K. Miller, E. Fetz, J. Ojemann, Sequential activation of premotor, primary somatosensory and primary motor areas in humans during cued finger movements, Clin. Neurophysiol. 126 (2016) 2150–2161.
[56] D. Wildgruber, M. Erb, U. Klose, W. Grodd, Sequential activation of supplementary motor area and primary motor cortex during self-paced finger movement in human evaluated by functional MRI, Neurosci. Lett. 227 (1997) 161–164.
[57] M. Annett, A classification of hand preference by association analysis, Br. J. Psychol. 61 (1970) 303–321.
[58] E. Sejdic, K.A. Lowry, J. Bellanca, S. Perera, M.S. Redfern, J.S. Brach, Extraction of stride events from gait accelerometry during treadmill walking, IEEE J. Transl. Eng. Heal. Med. 4 (2016) 1–11.
[59] J.M. Hausdorff, H.K. Edelberg, S.L. Mitchell, A.L. Goldberger, J.Y. Wei, Increased gait unsteadiness in community-dwelling elderly fallers, Arch. Phys. Med. Rehabil. 78 (1997) 278–283.
[60] R. Kitatani, K. Ohata, Y. Aga, Y. Mashima, Y. Hashiguchi, M. Wakida, A. Maeda, S. Yamada, Descending neural drives to ankle muscles during gait and their relationships with clinical functions in patients after stroke, Clin. Neurophysiol. 127 (2015) 1512–1520.
[61] K.K. Patterson, W.H. Gage, D. Brooks, S.E. Black, W.E. McIlroy, Evaluation of gait symmetry after stroke: a comparison of current methods and recommendations for standardization, Gait Posture 31 (2010) 241–246.
[62] J. Gwin, K. Gramann, S. Makeig, D. Ferris, Removal of movement artifact from high-density EEG recorded during walking and running, J. Neurophysiol. 103 (2010) 3526–3534.
[63] J.E. Kline, H.J. Huang, K.L. Snyder, D.P. Ferris, Isolating gait-related movement artifacts in eeg during human walking, J. Neural Eng. 12 (2015) 046022.
[64] R. Oostenveld, T. Oostendorp, Validating the boundary element method for forward and inverse EEG computations in the presence of a hole in the skull, Hum. Brain Mapp. 17 (2002) 179–192.
[65] J.T. Gwin, K. Gramann, S. Makeig, D.P. Ferris, EEG activity is coupled to gait cycle phase during treadmill walking, Neuroimage 54 (2011) 1289–1296.
[66] T. Jung, S. Makeig, C. Humphries, T. Lee, M. Mckeown, V. Iragui, T. Sejnowski, Removing electroencephalographic artifacts by blind source separation, Psychophysiology 37 (2000) 163–178.
[67] T. Jung, S. Makeig, M. Westerfield, J. Townsend, E. Courchesne, T. Sejnowski, Removal of eye activity artifacts from visual event-related potentials in normal and clinical subjects, Clin. Neurophysiol. 111 (2000) 1745–1758.
[68] A. Delorme, S. Makeig, EEGLAB : an open source toolbox for analysis of single-trial EEG dynamics including independent component analysis, J. Neurosci. Methods 134 (2004) 9–21.
[69] J. Wagner, T. Solis-Escalante, P. Grieshofer, C. Neuper, G.R. Müller-Putz, R. Scherer, Level of participation in robotic-assisted treadmill walking modulates midline sensorimotor EEG rhythms in able-bodied subjects, Neuroimage 63 (2012) 1203–1211.
[70] S. Pizzamiglio, U. Naeem, H. Abdalla, D.L. Turner, Neural correlates of single- and dual-task walking in the real world, Front. Hum. Neurosci. (2017) 11.
[71] D. Barthelemy, J.B. Nielsen, Corticospinal contribution to arm muscle activity during human walking, J. Physiol. (2010) 6.
[72] R. Nelson, Activity of monkey primary somatosensory cortical neurons changes prior to active movement, Brain Res. 406 (1987) 402–407.
[73] W. Szurhaj, E. Labyt, J. Bourriez, P. Kahane, P. Chauvel, F. Mauguiere, P. Derambure, Relationship between intracerebral gamma oscillations and slow potentials in the human sensorimotor cortex, Eur. J. Neurosci. 24 (2006) 947–954.
[74] W. Szurhaj, J. Bourriez, P. Kahane, P. Chauvel, F. Mauguière, P. Derambure, Intracerebral study of gamma rhythm reactivity in the sensorimotor cortex, Eur. J. Neurosci. 21 (2005) 1223–1235.
[75] B.M. de Jong, K.L. Leenders, A.M. Paans, Right parieto premotor activation related to limb independent antiphase movement, Cereb. Cortex (2002) 1213–1217.
[76] A. van der Hoorn, R.J. Renken, K.L. Leenders, B.M. de Jong, Parkinson-related changes of activation in visuomotor brain regions during perceived forward self-motion, PLoS One 9 (2014) e95861.
[77] T. Castermans, M. Duvinage, G. Cheron, T. Dutoit, About the cortical origin of the low delta and high gamma rhythms observed in EEG signals during treadmill walking, Neurosci. Lett. 561 (2014) 166–170.
[78] K. Snyder, J.E. Kline, H.J. Huang, D.P. Ferris, ICA of gait-related movement artifact recorded using EEG electrodes during treadmill walking, Front. Hum. Neurosci. (2015) 9.
[79] T. Lau, J. Gwin, D. Ferris, How many electrodes are really needed for eeg-based mobile brain imaging, J. Behav. Brain Sci. 2 (2012) 387–393.